A distance of 133–137 parsecs to the Pleiades star cluster

Xiaopei Pan[1], **M. Shao**[1] **& S. R. Kulkarni**[2]

[1]*Jet Propulsion Laboratory, California Institute of Technology, 4800 Oak Grove Drive, Pasadena, California 91109, USA*
[2]*Caltech Optical Observatories 105-24, California Institute of Technology, Pasadena, California 91125, USA*

Nearby 'open' clusters of stars (those that are not gravitationally bound) have played a crucial role in the development of stellar astronomy because, as a consequence of the stars having a common age, they provide excellent natural laboratories to test theoretical stellar models. Clusters also play a fundamental part in determining distance scales. The satellite Hipparcos[1] surprisingly found that an extensively studied open cluster—the Pleiades (also known as the Seven Sisters)—had a distance of $D = 118 \pm 4$ pc (refs 2, 3), about ten per cent smaller than the accepted value[4–6]. The discrepancy generated a spirited debate because the implication[7] was that either current stellar models were incorrect by a surprising amount or Hipparcos was giving incorrect distances. Here we report the orbital parameters of the bright double star Atlas in the Pleiades, using long-baseline optical/infrared interferometry. From the data we derive a firm lower bound of $D > 127$ pc, with the most likely range being $133 < D < 137$ pc. Our result reaffirms the fidelity of current stellar models.

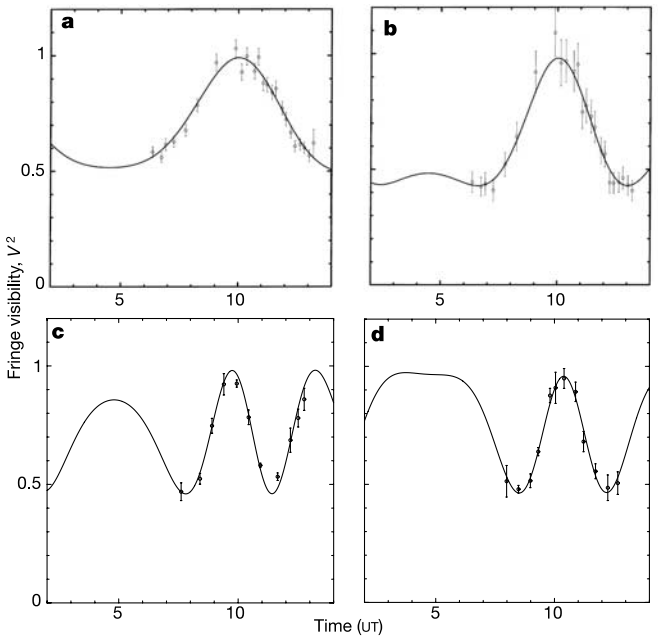

Figure 1 Fringe visibilities and model fits for Atlas. **a**, V^2 measured with the Mark III interferometer (marked by points with 1σ error bars) on UT 6 October 1992 at a mean wavelength of $\bar{\lambda} = 800$ nm. The best-fit model shown by the continuous curve corresponds to a binary with $S_\alpha = 5.07$ mas and $S_\delta = -0.46$ mas and component intensity ratio $r = 0.18$. **b**, As for **a** but at $\bar{\lambda} = 550$ nm. Model parameters are $S_\alpha = 4.96$ mas and $S_\delta = -0.43$ mas and $r = 0.202$. **c**, **d**, V^2 measurements from PTI obtained in the 2.2-μm band on UT 11 October 1998 (**c**) and UT 18 October 1998 (**d**). The corresponding model parameters are $S_\alpha = -6.83$ mas, $S_\delta = 7.77$ mas and $r = 0.18$ (for **c**) and $S_\alpha = -6.50$ mas, $S_\delta = 6.25$ and $r = 0.18$ (for **d**). The difference in magnitude, averaged over all PTI observations, is $\Delta K = 1.86 \pm 0.06$ and that for the Mark III data is $\Delta V = 1.68 \pm 0.07$. The errors were obtained by propagating the measurement errors.

Atlas (also known as HR1178 and HD23850) is a spectral type B8 giant star (luminosity class III) and, with visual magnitude $V = 3.62$ mag, is the second brightest star in the Pleiades. Although observed since 1903 (refs 8, 9), weak and broad spectral features made it difficult to demonstrate firmly that Atlas is a binary star. In 1974, lunar occultation observations[10] conclusively demonstrated its binary nature. However, given the limited occultation opportunities, the technique is not suitable for determining the orbital parameters.

During 1989–1992 we observed Atlas with the Mark III stellar interferometer[11] at optical wavelengths and easily resolved the binary system. Subsequently, between 1996–1999, observations in an infrared band were conducted with the Palomar Testbed Interferometer[12] (PTI). In Fig. 1 we show four nightly measurements of Atlas obtained from the Mark III interferometer and PTI. Each epoch was fitted to a binary model and the angular separations of the primary from the secondary are given in Table 1.

The separations obtained from our interferometric observations (Table 1) were fitted to a keplerian (elliptical) orbit and the resulting orbit (and the orbital parameters) is shown in Fig. 2. The lunar occultation observations[10,13,14] provide an independent check of our interferometric orbit. Thanks to the high precision of our orbital parameters, in particular the orbital period P_b, we can calculate the stellar separation for the epochs of the occultations over the past three decades. As can be seen from Table 2, the agreement, with one exception, is excellent.

The satellite Hipparcos can, in principle, detect the motion of the photocentre of a binary star with respect to other stars. The photocentric and visual orbits are related as follows:

$$a''_{\text{photo}} = a'' \times \frac{(q - r)}{(1 + q)(1 + r)} \quad (1)$$

where a''_{photo} and a'' (see Fig. 2) are the semi-major axis of the photocentric orbit and the visual orbit; q and r are the mass and intensity ratio of the secondary to that of the primary.

Table 1 **The angular separations in right ascension and declination between the primary and the secondary components**

JD 2,400,000+	S_α (mas)	$(M - C)_\alpha$ (mas)	S_δ (mas)	$(M - C)_\delta$ (mas)
Mark III Stellar Interferometer				
47872.7767	−7.50 ± 0.95	−0.34	12.1 ± 0.45	−0.33
48561.9051	4.20 ± 0.65	−0.17	−9.0 ± 0.15	0.02
48900.9468	4.68 ± 0.65	−0.11	−0.69 ± 0.15	−0.00
48901.9339	4.96 ± 0.65	0.24	−0.43 ± 0.15	0.02
48902.9230	4.44 ± 0.65	−0.20	−0.17 ± 0.15	0.04
Palomar Testbed Interferometer				
50359.8709	4.54 ± 0.63	0.12	0.38 ± 0.62	−0.11
50412.8662	−1.03 ± 0.63	0.20	11.05 ± 0.62	−0.26
50420.7811	−2.50 ± 0.63	−0.38	12.40 ± 0.62	0.05
51080.9480	−7.17 ± 0.58	0.04	10.96 ± 0.17	−0.13
51096.9303	−6.63 ± 0.55	0.15	7.84 ± 0.14	−0.17
51097.9347	−6.83 ± 0.51	−0.10	7.77 ± 0.14	−0.01
51104.9298	−6.50 ± 0.51	−0.20	6.25 ± 0.14	0.12
51105.8995	−6.35 ± 0.56	−0.12	6.03 ± 0.16	0.14
51127.8705	−3.93 ± 0.53	−0.10	−0.07 ± 0.14	0.04
51130.8410	−3.56 ± 0.54	−0.16	−0.83 ± 0.16	0.13
51154.7422	1.14 ± 0.53	0.46	−7.16 ± 0.16	−0.21
51155.7434	0.89 ± 0.54	0.04	−7.20 ± 0.16	−0.06
51470.8760	4.03 ± 0.51	-0.44	-8.93 ± 0.14	0.06
51480.9014	5.0 ± 0.51	−0.26	−8.31 ± 0.14	−0.11

S_α and S_δ were obtained by fitting the square of the fringe visibility function, V^2, to a binary model. See refs 26, 27 for examples of modelling of binary stars with interferometric data. For observations made with the Mark III stellar interferometer, the length of the baseline varied from 15.1 to 27.6 m and the visibility measurements were made in bands centred on 0.8, 0.55, 0.50 or 0.45 μm. For observations made with the Palomar Testbed Interferometer, the physical baseline was 109.8 m long and multiple channels centred on 2.2 μm were used. For these baselines, the inferred binary parameters are insensitive to the angular diameters of the components (which, on the basis of stellar theory, we set to 0.6 mas and 0.4 mas for Atlas A and Atlas B respectively). The separations were used to construct the visual orbit shown in Fig. 2. It is important to note that V^2 analysis yields the separation vector, but with an ambiguity of 180° in the position angle. We have chosen between the two orientations by trial and error, driven by the desire that the orbit smoothly connect between successive epochs. For each axis, the difference between the measurements (M) and the calculated or model (C) is shown in the column $M - C$.

We find the difference in V-band magnitudes of the two components is $\Delta V = 1.68 \pm 0.07$ (Fig. 1) which corresponds to $r = 0.212 \pm 0.014$. We obtain $a''_{\rm photo} = 0.32a''$ (for $q = 1$) and $a''_{\rm photo} = 0.25a''$ (for $q = 0.74 \pm 0.05$; see Fig. 3). Thus, $a''_{\rm photo}$ ranges from 4.21 to 3.24 milliarcseconds (mas). The small photocentric orbit is a challenging measurement for Hipparcos—as confirmed by the marginal (4σ) measurement, $a''_{\rm photo} = 4.23 \pm 0.97$ mas (ref. 1) as well as the non-detection of eccentricity. However, thanks to the better temporal sampling of the Hipparcos data, the orbital period of 290.7 ± 8.6 d is well-determined, and is consistent with our independently derived period (see Fig. 2).

Kepler's third law relates the total mass of the binary system, $M_{\rm tot}$, to a, the physical semi-major axis: $a^3 \propto M_{\rm tot}P_{\rm b}^2$. Noting that $a'' = a/D$, where D is the distance, simple error propagation of Kepler's third law yields:

$$V_{\rm R}(D) = 1/9 \times V_{\rm R}(M_{\rm tot}) + 4/9 \times V_{\rm R}(P_{\rm b}) + V_{\rm R}(a'') \qquad (2)$$

Here, $V_{\rm R}(x) \equiv (\sigma(x)/X)^2$ is the fractional variance of x, where X is the mean value and $\sigma^2(x)$ is the variance in x. As can be seen from Fig. 2, the fractional variance of $P_{\rm b}$ and a'' is 10^{-7} and 10^{-4}, respectively. Thus, even if the uncertainty in $M_{\rm tot}$ is 10%, given the high precision of our orbital parameters, the uncertainty on D will only be 3%.

To this end, we assumed the Hipparcos parallax and the isochrones of ref. 15 and derived the masses of the primary ($M_{\rm A}$) and secondary ($M_{\rm B}$) components. The mass estimates in conjunction with Kepler's third law yielded a new distance estimate. The procedure was repeated until the derived distance was the same as the assumed distance. The convergence was swift, requiring only three iterations. The convergence is rapid for the following reason. The mass is derived from the assumed luminosity ($L \propto D^2$) and the mass–luminosity relation, $L \propto M^{\beta}$; on the main sequence, $\beta \approx 3.8$. Combining with Kepler's third law we see that the derived distance $\propto M^{1/3} \propto D^{2/(3\beta)}$ is weakly dependent on the assumed distance.

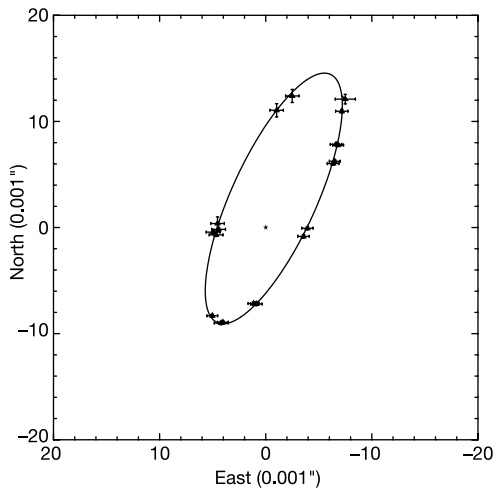

Figure 2 The visual orbit of Atlas. Each of the separation vectors displayed in Table 1 is represented by a triangle and is connected to the calculated positions by a short line. The symbol * refers to the primary star. The crosses indicate the formal 1σ errors (Table 1). A keplerian (elliptical) model was fitted to the separation vector in the framework of differential corrections (see ref. 26) to a binary orbit. The orbital elements of Atlas obtained from our observations are as follows: orbital period, $P_{\rm b} = 290.81 \pm 0.06$ d; epoch, $T_0 = {\rm JD}\ 2450582.8 \pm 1.5$ d; eccentricity, $e = 0.2457 \pm 0.006$; semi-major axis of the ellipse, $a'' = 12.94 \pm 0.11$ mas; and the three orientation angles, $i = 108.5° \pm 0.5°$, $\omega = 332.1° \pm 1.4°$ and $\Omega = 155.0° \pm 0.6°$. As an additional check on our orbital period, $P_{\rm b}$ (specifically the concern over ambiguities due to missed cycles), we explored the range 143 d to 590 d of orbital period and find the signal is strongest at $P_{\rm b} = 290.81 \pm 0.06$ d.

We find $M_{\rm B} = 3.57M_{\odot}$ (for $\tau_{\rm P} = 120$ Myr; here $\tau_{\rm P}$ is the age of the Pleiades cluster) or $M_B = 3.72M_{\odot}$ (for $\tau_{\rm P} = 90$ Myr) and $D = 136$ pc and an uncertainty of 2.6 pc arising from the uncertainty in $\tau_{\rm P}$. A strong lower limit of 127 pc is obtained by making the assumption $M_{\rm tot} > 2M_{\rm B}$. The results are summarized in Fig. 3. The uncertainty in D is comparable to the half-mass radius (of about 1.5 pc; refs 15, 16) for evolved stars in the Pleiades. Given that Atlas is either the second or third massive star in Pleiades it is likely that Atlas is in the core and not in the extended halo of Pleiades.

From our model we expect radial-velocity amplitudes of $K_{\rm A} = 27\ {\rm km\,s^{-1}}$ and $K_{\rm B} = 36\ {\rm km\,s^{-1}}$. With modern spectrographs it may be possible to obtain radial-velocity data with a precision of $1\ {\rm km\,s^{-1}}$ (preliminary observations by P. North, Ecole Polytechnique Fédérale de Lausanne). Such data, when combined with our interferometric model, can yield a distance estimate to the Pleiades that is accurate to 2%, independent of stellar models.

Our result reaffirms the traditional distance estimate[4–6] to the Pleiades and thus gives renewed confidence to the basic stellar model formulation used by astronomers. In particular, changing[18] the abundance of metals or that of He may result in a brighter main sequence but as noted above in equation (2), small changes in $M_{\rm tot}$ will result in even smaller changes in D.

Next, our parallax for Atlas is in disagreement with that obtained by Hipparcos. The mean Hipparcos parallax for the brightest (that is, the most massive) fifteen stars is 8.68 ± 0.21 mas, translating to a distance range of 107–124 pc (3σ). Thus we conclude that Hipparcos parallaxes for the Pleiades apparently suffer from an additional error of about 1 mas. The results presented here lend credence to the hypothesis[19] that Hipparcos measurements may be contaminated by systematic errors on small angular scales. Because such a conclusion would have important implications for Hipparcos parallaxes, it is imperative that accurate distances be derived for several other stars in the Pleiades.

As demonstrated by the work reported here, observations of a single binary can result in both an accurate and precise distance to the cluster. Interferometric observations, especially when combined with radial-velocity measurements, yield distance estimates that are independent of stellar models and extinction. With such distance estimates, stellar astronomers can focus on using open clusters as natural 'laboratories' in which to test their models and probe subtle effects due to rotation, stellar activity and convection.

Specialized modes of interferometry, in particular phase closure[20] and very-narrow-angle astrometry[21], offer even-higher-precision orbit determinations. Interferometry combined with precision radial-velocity measurements (particularly double-lined binaries[22]) can be used to test stellar models rigorously, given that both

Table 2 **Comparison of the interferometric model with lunar occultation observations**

JD 2,400,000+	Occultation		Interferometry		Calculated $\rho_{\rm p}$ (mas)	$\rho_{\rm l} - \rho_{\rm p}$ (mas)	Ref.
	$\phi_{\rm l}$(°)	$\rho_{\rm l}$ (mas)	ρ (mas)	θ(°)			
40221.6	56	6.2	9.23	181.6	5.4	0.8	10
41396.4	124	7.4	11.17	174.5	7.1	0.3	10
41724.7	49	4.0	15.28	161.2	5.8	−1.8	10
41397.1	93.7	2.5	11.27	−5.9	1.9	0.6	13
46988.2	21.1	6.8	15.29	−26.5	10.3	−3.5	14
48307.8	294.4	6.2	6.43	122.2	6.4	−0.2	14

JD, the epoch (Julian Day) of the lunar occultations. $\phi_{\rm l}$ is the position angle of the lunar limb at the time of occultation. $\rho_{\rm l}$ is the projected binary separation inferred from the occultation observations. The polar coordinates of the separation between the primary and secondary components extrapolated from the binary model presented in Fig. 2 are ρ and θ (the angle measured from North towards East). Our orbital model has precision sufficient to extrapolate from the 1990s to the period 1968–1991 over which the lunar occultation observations were conducted. The calculated projected separation is $\rho_{\rm p} = \rho\cos(\theta - \phi_{\rm l})$. Our reading of the literature suggests that the typical error in lunar occultation measurements is about 1 mas. As can be seen from the last column, our model can account for the lunar occultation observations within errors. A measurement on 29 December 1971 (ref. 13) was not used, given the cautionary statements made by the authors. Lunar occultation experiments[14] also yield the magnitude difference: $\Delta V = 1.6 \pm 0.2$ mag and $\Delta K = 1.80 \pm 0.21$ mag. These are consistent with our results in Fig. 1.

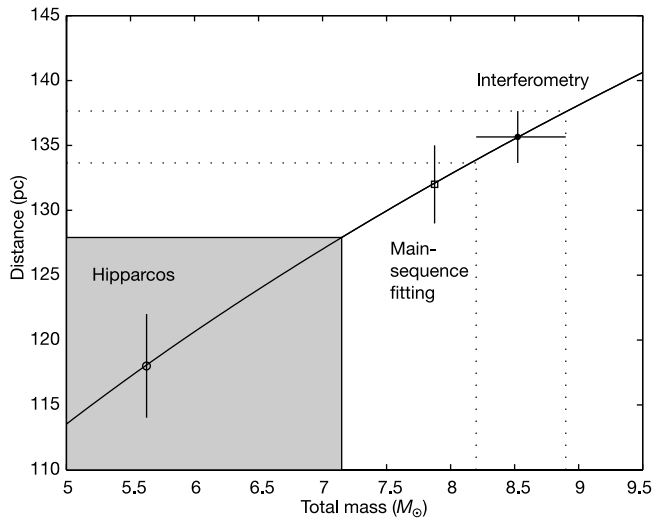

Figure 3 Mass–distance relationship for Atlas. Using the measured angular length of a'' and P_b (see Fig. 2), Kepler's third law allows us to relate the distance D to $M_{tot} = M_A + M_B$ of the binary system (black curve). The final uncertainty in D is dominated by uncertainty in M_{tot} (see below) and for this reason the black curve is shown without the width arising from uncertainties in the orbital parameters. We derive the masses of the components by comparing their observed V magnitudes (Fig. 1) against the stellar models of ref. 15. Here and throughout the text, following ref. 4, we assume a mean interstellar extinction of $E_{B-V} = 0.04$ mag. We find $M_B = 3.57M_\odot$ (for assumed Pleiades cluster age, $\tau_P = 120$ Myr) or $M_B = 3.72M_\odot$ (for $\tau_P = 90$ Myr). The mass of the secondary (apart from the uncertainty in the assumed age) is robust because on the main sequence the luminosity increases steeply with mass ($L \propto M^\beta$ with $\beta \approx 3.8$) and this relation, when combined with Kepler's third law, makes the derived distance almost independent of the assumed mass (see the discussion following equation (2)). The star Maia, presumably a single star with $V = 3.87$, is a twin of Atlas A but with well-determined colours. Using isochrones that allow for convective overshoot[15], estimates for M_A vary from $4.62M_\odot$ (for $\tau_P = 120$ Myr) to $5.19M_\odot$ (for $\tau_P = 90$ Myr); isochrones supplied by D. VandenBerg (personal communication) clearly favour the latter age and $M_A = 5.19M_\odot$. Thus, $M_{tot} = 8.2$ to $8.9M_\odot$, which leads to D being uncertain from 133.9 pc to 137.6 pc (the dotted lines). Black circle, the arithmetic mean of these two estimates. The error bar is ± 2.6 pc, arising from the uncertainty in M_{tot}. Square, the distance to the Pleiades based on main-sequence fitting[5]. White circle, the Hipparcos distance estimate[2,3] of 118 ± 4 pc. Neither technique involves the masses of the components of Atlas and hence no horizontal error bars are shown. As argued above, at the very minimum, $M_{tot} > 2M_B > 7.14M_\odot$, which translates to $D > 127$ pc. The shaded region marks the parameter space excluded by our observations.

components are expected to lie on exactly the same isochrone. Radial-velocity studies[23], lunar occultation[24] and photometric[25] observations have revealed many binaries in the Pleiades. The availability of new-generation high-resolution spectrographs and the recent commissioning of powerful interferometers at the Keck Observatory and the Very Large Telescope facility are expected to facilitate such testing of stellar models. □

Received 29 September; accepted 11 December 2003; doi:10.1038/nature02296.

1. Perryman, M. A. C. *et al.* The HIPPARCOS Catalogue. *Astron. Astrophys.* **323,** L49–L52 (1997).
2. Mermilliod, J.-C., Turon, C., Robichon, N., Arenou, F. & Lebreton, Y. in *ESA SP-402: Hipparcos—Venice'97* (eds Perryman, M. A. C. & Bernacca, P. L.) 643–650 (European Space Agency, Paris, 1997).
3. van Leeuwen, F. & Hansen Ruiz, C. S. in *ESA SP-402: Hipparcos—Venice'97* (eds Perryman, M. A. C. & Bernacca, P. L.) 689–692 (European Space Agency, Paris, 1997).
4. Meynet, G., Mermilliod, J.-C. & Maeder, A. A New dating of galactic open clusters. *Astron. Astrophys. Suppl. Ser.* **98,** 477–504 (1993).
5. Pinsonneault, M. H., Stauffer, J., Soderblom, D. R., King, J. R. & Hanson, R. B. The problem of HIPPARCOS distances to open clusters. I. Constraints from multicolor main-sequence fitting. *Astrophys. J.* **504,** 170–191 (1998).
6. Gatewood, G., de Jonge, J. K. & Han, I. The Pleiades, MAP-based trigonometric parallaxes of open clusters. V. *Astrophys. J.* **533,** 938–943 (2000).
7. Paczynski, B. The distance to Pleiades. *Acta Astron.* **53,** 209–211 (2003).
8. Abt, H. A., Barnes, R. C., Biggs, E. S. & Osmer, P. S. The frequency of spectroscopic binaries in the Pleiades. *Astrophys. J.* **142,** 1604–1615 (1965).
9. Pearce, J. A. & Hill, G. Four suspected spectroscopic binaries in the Pleiades. *Publ. Astron. Soc. Pacif.* **83,** 493–495 (1971).
10. McGraw, J. T., Dunham, D. W., Evans, D. S. & Moffet, T. J. Occultations of the Pleiades: photoelectric observations at Tonantzintla with a discussion of the duplicity of Atlas. *Astron. J.* **79,** 1299–1303 (1974).
11. Shao, M., Colavita, M. M., Hines, B. E., Staelin, D. H. & Hutter, D. J. The Mark III stellar interferometer. *Astron. Astrophys.* **193,** 357–371 (1988).
12. Colavita, M. M. *et al.* The Palomar testbed interferometer. *Astrophys. J.* **510,** 505–521 (1999).
13. de Vegt, C. & Gehlich, U. K. Results of photoelectric lunar occultation observations obtained at the Hamburg Observatory during 1969–1973. *Astron. Astrophys.* **48,** 245–252 (1976).
14. Meyer, C., Rabbia, Y., Froeschle, M., Helmer, G. & Amieux, G. Observations of lunar occultations at Observatoire de la Cote d'Azur. *Astron. Astrophys. Suppl. Ser.* **110,** 107–123 (1995).
15. Ventura, P., Zeppieri, A., Mazzitelli, I. & D'Antona, F. Full spectrum of turbulence convective mixing: I Theoretical main sequences and turn-off for 0.6–15 $M_\odot$. *Astron. Astrophys.* **334,** 953–968 (1998).
16. Raboud, D. & Mermilliod, J.-C. Investigation of the Pleiades cluster. IV. The radial structure. *Astron. Astrophys.* **329,** 101–114 (1998).
17. Pinfield, D. J., Jameson, R. F. & Hodgkin, S. T. The mass of the Pleiades. *Mon. Not. R. Astron. Soc.* **299,** 955–964 (1998).
18. Castellani, V., Degl'Innocenti, S., Prada Moroni, P. G. & Tordiglione, V. Hipparcos open clusters and stellar evolution. *Mon. Not. R. Astron. Soc.* **334,** 193–197 (2002).
19. Narayanan, V. K. & Gould, A. Correlated errors in HIPPARCOS parallaxes toward the Pleiades and the Hyades. *Astrophys. J.* **523,** 328–339 (1999).
20. Shao, M. & Colavita, M. M. Long-baseline optical and infrared stellar interferometry. *Annu. Rev. Astron. Astrophys.* **30,** 457–498 (1992).
21. Lane, B. F. & Muterspaugh, M. W. Differential astrometry of sub-arcsecond scale binaries at the Palomar testbed interferometer. *Astron. J.* **125,** 1623–1628 (2003).
22. Giannuzzi, M. A. The spectroscopic binary HD 23642 and the distance of the Pleiades. *Astron. Astrophys.* **293,** 360–362 (1995).
23. Mermilliod, J.-C., Rosvick, J. M., Duquennoy, A. & Mayor, M. Investigation of the Pleiades cluster. II—Binary stars in the F5-K0 spectral region. *Astron. Astrophys.* **265,** 513–526 (1992).
24. Richichi, A., Calamai, G. & Leinert, C. New binary stars discovered by lunar occultations. *Astron. Astrophys.* **286,** 829–837 (1994).
25. Torres, G. Discovery of a bright eclipsing binary in the Pleiades cluster. *Inform. Bull. Variable Stars* **5402,** 1–3 (2003).
26. Pan, X. P. *et al.* Apparent orbit of the spectroscopic binary β *Arietis* with the Mark III stellar interferometer. *Astrophys. J.* **356,** 641–645 (1990).
27. Hummel, C. A. *et al.* The spectroscopic binary eta Andromedae: Determination of the orbit by optical interferometry. *Astron. J.* **106,** 2486–2492 (1993).

Acknowledgements We thank other members of the PTI and Mark III teams and especially A. Boden and B. Lane for a careful reading. We gratefully acknowledge discussions with N. Reid, R. M. Rich, D. Sasselov, J. Stauffer, J. Tomkin and D. VandenBerg. We extensively used the SIMBAD database of astronomical papers and are grateful to CDS, France, and NASA for maintaining this system. The research described in this paper was primarily carried out at the Jet Propulsion Laboratory, California Institute of Technology, under a contract with the National Aeronautics and Space Administration. S.R.K.'s research is supported by NSF and NASA.

Competing interests statement The authors declare that they have no competing financial interests.

Correspondence and requests for materials should be addressed to S.R.K. (srk@anju.caltech.edu).

The microscopic nature of localization in the quantum Hall effect

S. Ilani[1]*, J. Martin[1], E. Teitelbaum[1], J. H. Smet[2], D. Mahalu[1], V. Umansky[1] & A. Yacoby[1]

[1]*Department of Condensed Matter Physics, Weizmann Institute of Science, Rehovot 76100, Israel*
[2]*Max-Planck-Institut für Festkörperforschung, D-70569 Stuttgart, Germany*

* Present address: Laboratory of Atomic and Solid State Physics, Cornell University, Ithaca, New York 14853, USA

The quantum Hall effect arises from the interplay between localized and extended states that form when electrons, confined to two dimensions, are subject to a perpendicular magnetic field[1]. The effect involves exact quantization of all the electronic transport properties owing to particle localization. In the conventional theory of the quantum Hall effect, strong-field localization is associated with a single-particle drift motion of electrons along